

Linearization of the Hoek and Brown rock failure criterion for tunnelling in elasto-plastic rock masses

Rafael Jimenez^{a,b,*}, Alcibiades Serrano^b, Claudio Olalla^b

^aDepartment of Civil and Environmental Engineering, Imperial College London, The Skempton Building, Room 335, London SW7 2AZ, UK

^bETS Caminos, C. y P, Universidad Politecnica de Madrid, Spain

Received 3 November 2007; accepted 5 December 2007

Available online 29 February 2008

Abstract

We present a novel methodology for estimation of equivalent Mohr–Coulomb strength parameters that can be used for design of supported tunnels in elasto-plastic rock masses satisfying the non-linear empirical Hoek–Brown failure criterion. We work with a general adimensional formulation of the Hoek–Brown failure criterion in the space of normalized Lambe’s variables for plane stress, and we perform linearization considering the stress field in the plastic region around the tunnel. The procedure is validated using analytical solutions to a series of benchmark test cases. Numerical solutions are also employed to validate the procedure in cases for which analytical solutions are not available. Results indicate that the stress field in the plastic region around the tunnel, as well as the linearization method employed and the quality of the rock mass, has a significant impact on computed estimates of equivalent Mohr–Coulomb strength parameters. Results of numerical analyses also show that our proposed linearization method can be employed to estimate loads and moments on the tunnel support system. We recommend the equating model responses (EMR) method to compute equivalent Mohr–Coulomb strength parameters when the tunnel support pressure is accurately known, and we further show that our newly introduced linearization method can be employed as an alternative to the best fitting in the existing stress range (BF_e) and best fitting in an artificial stress range (BF_a) methods, providing performance estimates that are generally better than estimates of the BF_e and BF_a methods when differences with the response of the Hoek–Brown rock mass are of engineering significance (say more than 10%).
© 2008 Elsevier Ltd. All rights reserved.

Keywords: Mohr–Coulomb; Rock mass strength; Non-linear; Plasticity

1. Introduction

Rock mass strength is a non-linear function of stress level. The empirical Hoek–Brown (HB) failure criterion (see e.g., [1–5]) accounts for this observation, and it is the criterion most commonly employed to characterize failure of rock masses in tunnelling projects. The HB non-linear failure criterion is often linearized in practical applications to obtain an “equivalent” linear failure criterion in terms of Mohr–Coulomb (MC) parameters. One reason to explain such interest to linearize the HB failure criterion is that certain software packages commonly employed for tunnel

design do not provide the HB failure criterion [6]. In addition, geotechnical strength parameters have been traditionally expressed in terms of angle of friction, ϕ , and cohesion, c , values, which makes many practitioners more used to work with the equivalent MC parameters than with the original HB parameters. Furthermore, although (almost) exact closed-form solutions to compute stresses and displacements of axisymmetric tunnels in rock masses with the HB failure criterion are now available (see e.g., [7–9]), equivalent MC parameters can also be employed by tunnel designers to compute fast approximate estimates—suitable, for instance, for preliminary design—of tunnel performance using the convenient rigorous graphical solutions for MC rock masses developed by Carranza-Torres [10].

Hoek and Brown [4] propose a method to linearize the HB failure criterion using eight simulated triaxial tests

*Corresponding author at: Department of Civil and Environmental Engineering, Imperial College London, The Skempton Building, Room 335, London SW7 2AZ, UK. Tel.: +44 2075946001; fax: +44 2075945934.

E-mail address: r.jimenez@imperial.ac.uk (R. Jimenez).

conducted at constant increments of the confining pressure, σ_3 , within the interval $0 < \sigma_3 < 0.25\sigma_{ci}$, where σ_{ci} is the uniaxial compressive strength of the intact rock. (For shallow tunnels, the upper bound of $0.25\sigma_{ci}$ was later increased to the value of the overburden pressure [6].) Values of equivalent MC parameters, c and ϕ , are then computed by least squares fitting of a straight line to the results of such simulated triaxial tests. More recently, Hoek et al. [5] propose to linearize in the $\sigma_1 - \sigma_3$ stress space, equating the areas covered by the HB and the MC criteria for the stress interval $\sigma_t < \sigma_3 < \sigma_{3,max}$, where σ_t is the tensile strength of the rock mass and $\sigma_{3,max}$ is the maximum confining stress level considered.

Note, however, that such stress ranges do not agree with the actual stress state around the tunnel; instead, they are artificial stress intervals, defined to provide equivalent parameters for each individual tunnel considered [5,6]. In other words, methods described above consider only partially the stress state in the rock mass when performing the linearization and, for instance, they do not consider the effect of the tunnel support pressure on the linearization results. The consideration of the actual stress field around the tunnel, however, is a crucial aspect of the linearization problem, as the non-linear failure criterion can only be substituted by a linear criterion, with an acceptable error, if an adequate and realistic stress range is considered. This observation led to recent research to estimate equivalent MC parameters for supported tunnels in rock and, for instance, Sofianos and Nomikos [6] (see also [11,12]) propose a method to linearize the HB failure criterion in which the real stress field within the plastic region around the tunnel (including the influence of the tunnel support pressure) is considered.

In this work we present a novel methodology for the estimation of equivalent MC strength parameters that can be used for design of supported tunnels in elasto-plastic rock masses with the HB failure criterion. To that end, we work with a general adimensional formulation of the HB failure criterion in the space of normalized Lambe's stress variables developed by Serrano et al. [13], and we perform a simple linearization procedure in which the actual stress field in the plastic region around the tunnel is considered.

2. Estimation of equivalent strength parameters

2.1. An adimensional formulation of the HB failure criterion

The generalized HB failure criterion provides empirical estimates of rock mass strength. It can be expressed as (see e.g., [4,5])

$$\sigma_1 = \sigma_3 + \sigma_{ci} \left(m_b \frac{\sigma_3}{\sigma_{ci}} + s \right)^a, \quad (1)$$

where σ_1 and σ_3 are the major and minor principal stresses; σ_{ci} is the uniaxial compressive strength of the intact rock; s and a are parameters that depend on the quality of the rock

mass (as expressed, for instance, by the Geological Strength Index, GSI); and m_b is a parameter that depends on the type of rock and on the quality of the rock mass.

The failure criterion of Eq. (1) can also be expressed in terms of Lambe's variables for plane strain ($p = (\sigma_1 + \sigma_3)/2$; $q = (\sigma_1 - \sigma_3)/2$). We obtain the following general adimensional equation [13]:

$$p_0^* = (1 + (1 - a)q^{*k})q^*, \quad (2)$$

where p^* and q^* are normalized Lambe variables (i.e., $p^* = p/\beta$; $q^* = q/\beta$); p_0^* is defined as $p_0^* = p^* + \zeta$; and k , β , ζ are parameters that depend on the parameters of the generalized HB failure criterion:

$$k = \frac{1 - a}{a}, \quad (3)$$

$$\beta = A\sigma_{ci}, \quad (4)$$

$$\zeta = \frac{s}{m_b A}, \quad (5)$$

where A is defined as $A^k = m_b(1 - a)/2^{1/a}$.

In this work we have employed the last available version of the HB failure criterion [5], with a value of the damage factor of $D = 0$. Eqs. (2)–(5), however, should be valid even if the procedures to compute m_b , s , and a change in future versions of the HB criterion, as long as the overall form of the HB criterion is maintained. (Formulas to compute m_b , a and s usually change for successive versions of the HB criterion, but the overall form of the expression in Eq. (1) has been maintained, for more than 25 years, since the early versions of the criterion.)

2.2. A simple linearization procedure

Fig. 1 shows a circular supported tunnel in an elasto-plastic rock mass that satisfies the HB failure criterion. The in situ stress field is considered hydrostatic with $\sigma_1 = \sigma_3 = \sigma_0$, and the tunnel support pressure is σ_A . Fig. 1 also shows two points (A and B) at the boundaries of the plastic region formed around the tunnel. Stresses at points A and B define the range of stresses at the zone around the tunnel where the rock mass has reached its ultimate strength and, therefore, where the strength criterion considered is significant.

Point A is located at the tunnel lining, where the support pressure acts. We will assume that the support pressure at A is the minor principal stress at that point, as that is the most common case in practice. (Note, however, that there might be cases in which the internal pressure at the lining is in fact the major principal stress; e.g., in pressurized hydraulic tunnels.) Point B is located at the interface between the plastic region around the tunnel and the elastic region, where the rock mass did not reach its peak strength. We use σ_B to denote the radial stress acting at the elasto-plastic interface at point B . (σ_B is also the critical pressure; i.e., the critical support pressure at the tunnel lining needed

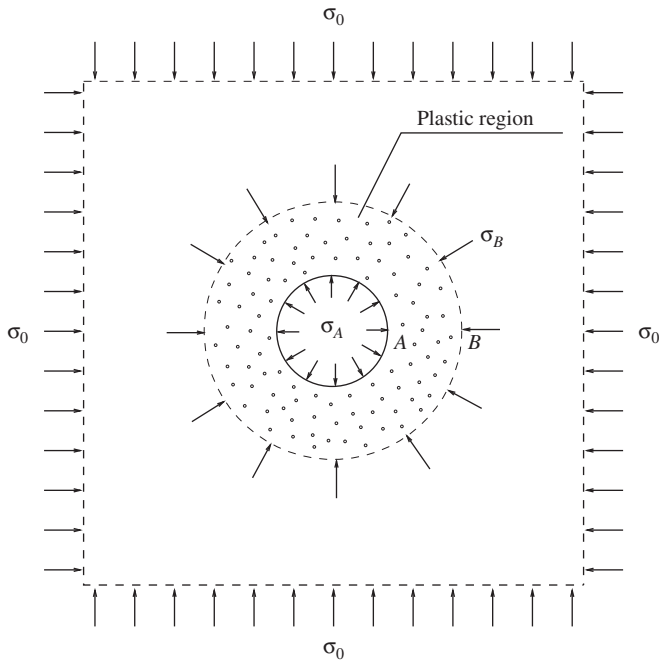


Fig. 1. Plastic region around a tunnel.

to avoid the formation of a plastic region around the tunnel [6].)

From elasticity theory we know that Lambe’s p variable must remain constant within the elastic region (this observation is also valid for point B , which is at the boundary of the elastic region). Therefore, as shown in Fig. 2(a), the (normalized) deviatoric stress at failure at point B , q_B^* , can be obtained following the vertical arrow from $p_B^* = \sigma_0^*$ up to its intersection with the HB failure envelope. (Fig. 2(a) also shows the Mohr’s circles that represent the stress states at points A and B ; i.e., at the boundaries of the plastified region around the tunnel.) The approach to obtain the stress state at failure at point A is slightly different. At point A , we know that the support pressure at the tunnel lining corresponds to the minor principal stress $\sigma_3 = \sigma_A$. Therefore, its deviatoric stress at failure, q_A^* , can be computed following the arrow at 45° from $p_A^* = \sigma_A^*$ up to its intersection with the HB failure envelope. (See Fig. 2(a).)

To perform the linearization of the HB criterion that provides equivalent MC parameters, we start by plotting a straight line passing through points A and B . Such line can be defined as a function of its slope angle, θ_{AB} , and of its ordinate at the origin, C_{AB}^* (see Fig. 2(b)). Such linearization is conservative, as it provides a lower bound of strength values; that is, the strength values computed in this way are smaller than those provided by the HB criterion for all stresses between p_A and p_B . To improve the computed predictions, we also plot a straight line parallel to the line from A to B that passes through M , which is the point whose deviatoric stress is the mean of the deviatoric stresses at points A and B (that is, $q_M^* = (q_A^* + q_B^*)/2$; see Fig. 2(b)). This additional line, not shown in Fig. 2(b) to

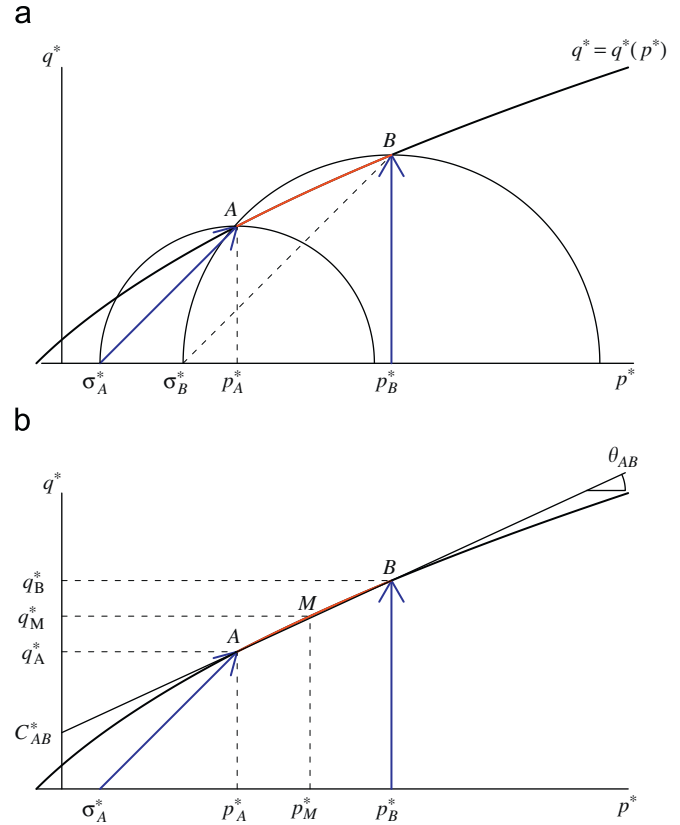


Fig. 2. Example representation of stresses acting at the plastified region around the tunnel and procedure for linearization of the Hoek–Brown - failure criterion within such stress range. (a) Mohr’s circles representing the stress state at the boundaries of the plastic region around the tunnel. (b) Linearization of the Hoek–Brown failure criterion considering the stress state within the plastic region.

maintain clarity, would have a slope of value $\theta_M = \theta_{AB}$ and an ordinate at the origin of value C_M^* . The equivalent instantaneous friction angle can then be computed as

$$\sin \phi = \tan \theta_{AB}. \tag{6}$$

To compute the equivalent cohesion we use an ordinate at the origin of intermediate value between C_{AB}^* and C_M^* ; i.e., $C^* = (C_{AB}^* + \zeta_C^* (C_M^* - C_{AB}^*))$, where $0.0 \leq \zeta_C^* \leq 1.0$. (In Section 3 we present a sensitivity analysis to compute the “optimum” value of ζ_C^* ; results in this paper are computed using $\zeta_C^* = 0.60$.) The equivalent cohesion can then be computed as

$$c = \frac{\beta C^*}{\cos \phi}. \tag{7}$$

Note that, for the sake of clarity, we describe the proposed linearization method using a simple graphical procedure, as closed-form expressions to compute q^* from Eq. (2) are not available in general. (They are only available for certain values of a such as, for instance, $a = \frac{1}{2}$.) Routines to compute exact values of q_A^* and q_B^* , however, can be easily implemented using standard software packages for numerical analysis; similarly, the values of θ_{AB} , and of C_{AB}^* and C_M^* can be easily computed

(using basic geometry) once the coordinates of points $A \equiv (p_A^*, q_A^*)$ and $B \equiv (p_B^*, q_B^*)$ are known in Fig. 2. That is the approach that we follow to compute the results presented in this work.

3. Example analyses

3.1. Influence of rock mass quality and of support pressure

Fig. 3 shows equivalent MC parameters computed using the linearization procedure described in Section 2 for rock masses of different qualities and for different values of the

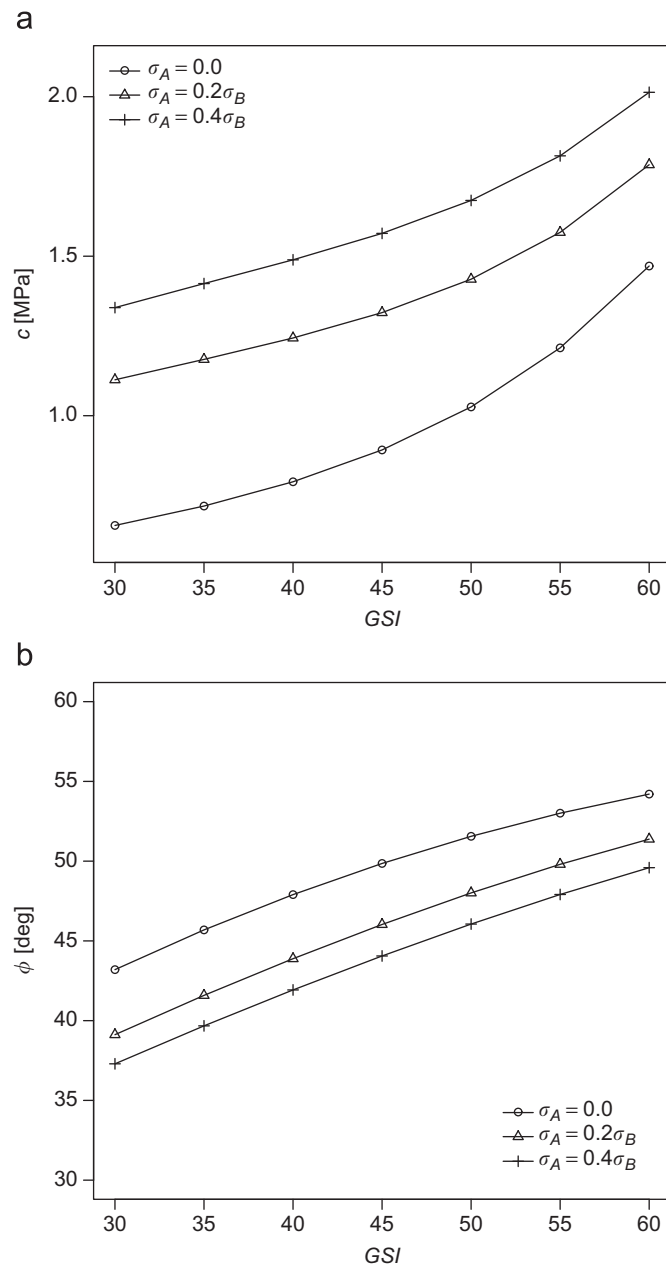


Fig. 3. Equivalent MC parameters for different qualities of the rock mass and different levels of support pressure. (Computed for $m_i = 12$, $\sigma_{ci} = 80$ MPa, and $\sigma_0 = 10$ MPa.) (a) Cohesion vs GSI, (b) friction angle vs GSI.

tunnel support pressure. (Tunnel support pressure is expressed as a function of the critical pressure, σ_B .) In all cases, we have considered a rock mass with $m_i = 12$ and $\sigma_{ci} = 80$ MPa. The natural in situ stress field is considered hydrostatic with $\sigma_0 = 10$ MPa.

Fig. 3 shows that the equivalent MC parameters heavily depend on the quality of the rock mass and on the tunnel support pressure. It is also observed that, given a constant GSI value, the equivalent cohesion increases as support pressure increases, whereas the equivalent friction angle decreases as support pressure increases. Similarly, as expected for a given constant value of the tunnel support pressure, results indicate that the equivalent cohesion and the equivalent friction angle increase as the rock mass quality increases.

3.2. Analytical solutions of tunnel response

We have also compared equivalent MC strength parameters computed with our linearization procedure presented in Section 2 with MC parameters computed using other linearization methods. In particular, we have compared them with the BFa (“best fitting in an artificial stress range”) method proposed by Hoek et al. [5]; and with the EMR (“equating model responses”) and BFe (“best fitting in the existing stress range”) methods proposed by Sofianos and Nomikos [6]. Table 1 lists equivalent MC parameters computed with these methods in several benchmark test cases. For ease of comparison, benchmark test cases listed in Table 1 are identical to the validation cases considered by Sofianos and Nomikos [6] (see Table 2 in [6]). Following the notation in [6], sub-case (a) corresponds to the unsupported case (i.e., $\sigma_A = 0.0$), whereas sub-case (b) corresponds to a case with a supported tunnel with support pressure $\sigma_A = 0.2\sigma_B$.

Table 2 lists differences (expressed as percentage) between the equivalent MC parameters computed with the linearization method proposed herein and MC parameters computed with the BFe, EMR, and BFa linearization methods. Results show that cohesion values computed with our linearization method tend to be lower than those computed with the BFe method (up to 65%) and the EMR method (up to 30%); and that equivalent friction angles computed with our method tend to be higher (up to 10%) than those computed with the BFe and EMR methods. (Differences tend to higher for cases without tunnel support and, in general, for cases with lower GSI values.) Results also show that differences with the results of our method tend to be significantly higher for the BFa method (which does not consider the actual stress field around the tunnel) than for the EMR and BFe methods.

In Table 3 we study the predictions of performance (with respect to radius of the plastic region, r_e , critical support pressure, p_e , and radial convergence, u) using analytical solutions for the original HB rock masses, and we compare such predictions with those computed using

Table 1

Equivalent Mohr–Coulomb parameters computed with different linearization methods using the benchmark test cases presented by Sofianos and Nomikos [6]

Case	Hoek–Brown rock mass			Mohr–Coulomb rock mass							
	m_b	s	a	BF ^e ^a		EMR ^a		BF ^a ^a		This work	
				c (MPa)	ϕ (deg)	c (MPa)	ϕ (deg)	c (MPa)	ϕ (deg)	c (MPa)	ϕ (deg)
1(a)	2.0121	3.87E – 03	0.506	1.117	50.62	1.185	49.32	1.707	43.89	1.009	51.56
1(b)	2.0121	3.87E – 03	0.506	1.339	48.73	1.444	47.58	1.707	43.89	1.291	49.09
2(a)	0.6567	4.19E – 04	0.522	0.102	46.18	0.106	44.96	0.144	40.97	0.089	47.30
2(b)	0.6567	4.19E – 04	0.522	0.127	44.06	0.138	42.88	0.144	40.97	0.119	44.66
3(a)	0.6567	4.19E – 04	0.522	0.720	21.77	0.594	21.43	0.585	23.98	0.455	24.05
3(b)	0.6567	4.19E – 04	0.522	1.004	19.48	1.089	18.51	0.585	23.98	0.950	19.87
4(a)	6.6746	6.22E – 02	0.501	1.888	57.39	1.953	56.65	2.651	49.56	1.875	57.50
4(b)	6.6746	6.22E – 02	0.501	1.950	56.80	2.006	56.22	2.651	49.56	1.942	56.86
5(a)	4.4695	2.05E – 02	0.502	1.098	48.74	1.159	47.42	1.597	42.77	0.970	49.87
5(b)	4.4695	2.05E – 02	0.502	1.343	46.67	1.453	45.47	1.597	42.77	1.295	47.04
6(a)	0.5514	1.38E – 04	0.544	0.073	27.62	0.059	27.33	0.068	28.37	0.047	29.73
6(b)	0.5514	1.38E – 04	0.544	0.103	25.19	0.112	24.13	0.068	28.37	0.099	25.50
7(a)	0.6625	2.15E – 04	0.533	0.085	42.37	0.081	41.49	0.116	38.42	0.065	44.04
7(b)	0.6625	2.15E – 04	0.533	0.115	39.88	0.126	38.68	0.116	38.42	0.110	40.25
8(a)	0.6625	2.15E – 04	0.533	0.645	19.40	0.496	19.28	0.495	22.03	0.391	21.54
8(b)	0.6625	2.15E – 04	0.533	0.904	17.32	0.979	16.44	0.495	22.03	0.861	17.62
9(a)	0.4018	4.54E – 05	0.585	0.057	22.31	0.039	22.37	0.046	24.14	0.036	23.77
9(b)	0.4018	4.54E – 05	0.585	0.081	20.34	0.088	19.51	0.046	24.14	0.078	20.52

BF^e represents the “best fitting in the existing stress range” method [6]; EMR represents the “equating model responses” method [6]; and BF^a represents the “best fitting in an artificial stress range” method [5].

^aValues reproduced from Sofianos and Nomikos [6].

Table 2

Differences (expressed as percentage) between values of cohesion and friction angle computed with the linearization method proposed in this work and those computed using linearization methods proposed by Hoek et al. [5] and Sofianos and Nomikos [6]

Case	Mohr–Coulomb rock mass					
	BF ^e		EMR		BF ^a	
	δc (%)	$\delta \phi$ (%)	δc (%)	$\delta \phi$ (%)	δc (%)	$\delta \phi$ (%)
1(a)	10.74	–1.82	17.48	–4.34	69.23	–14.87
1(b)	3.71	–0.74	11.84	–3.09	32.21	–10.60
2(a)	15.14	–2.37	19.65	–4.95	62.54	–13.39
2(b)	6.33	–1.35	15.54	–3.99	20.56	–8.27
3(a)	58.17	–9.48	30.49	–10.89	28.51	–0.29
3(b)	5.68	–1.95	14.63	–6.83	–38.42	20.70
4(a)	0.69	–0.18	4.15	–1.47	41.38	–13.80
4(b)	0.41	–0.11	3.30	–1.13	36.51	–12.84
5(a)	13.22	–2.26	19.51	–4.91	64.67	–14.23
5(b)	3.67	–0.78	12.16	–3.33	23.28	–9.07
6(a)	54.42	–7.09	24.81	–8.06	43.85	–4.56
6(b)	4.30	–1.21	13.42	–5.37	–31.14	11.26
7(a)	31.32	–3.78	25.14	–5.78	79.22	–12.75
7(b)	4.64	–0.92	14.65	–3.90	5.55	–4.54
8(a)	65.12	–9.94	26.98	–10.50	26.72	2.27
8(b)	5.05	–1.70	13.77	–6.69	–42.48	25.04
9(a)	56.43	–6.14	7.03	–5.88	26.24	1.56
9(b)	3.54	–0.88	12.49	–4.92	–41.20	17.64

equivalent MC parameters computed using our linearization method as well as the BF^e, EMR, and BF^a methods. For ease of comparison of results, the same benchmark test

cases considered by Sofianos and Nomikos [6] have also been employed in this case. The response of the rock mass with equivalent MC parameters has been computed using the expressions of Carranza-Torres [10]. (Instead of using the expressions previously developed by Duncan Fama [14]; this explains the slight differences between results presented in Table 3 of this note and in Table 4 of [6].)

In Table 4 we present the relative errors (expressed as percentage) between performance predictions computed considering the HB rock mass and also equivalent MC parameters for different linearization methods. Table 5 lists the number of cases, out of 42 cases considered, in which the relative errors of predictions of plastic radius, critical support pressure, or radial convergence (when compared to the HB rock mass predictions) are greater than 5%, 10%, and 20%.

Results indicate that the EMR method [6] provides the smallest relative errors with respect to plastic radius, critical support pressure, and radial convergence. Such excellent results, however, have been computed for cases in which support pressures are known with high accuracy; the agreement is not so good when the estimation of the support pressure is poor, as it often happens in real tunnelling projects. In fact, Sofianos and Nomikos [6] recommend to use the BF^e or the BF^a methods as an alternative to the EMR method when the support pressure is not known with sufficient accuracy.

Based on our results, we argue that our newly proposed linearization procedure can be employed as a simple and

Table 3
Estimates of radius of the plastic region, critical pressure, and radial convergence of several benchmark test tunnel cases

Case	ψ (deg)	HB rock mass ^a			Mohr–Coulomb rock mass											
		r_e (m)	p_e (MPa)	u (mm)	BFe			EMR			BFa			This work		
					r_e (m)	p_e (MPa)	u (mm)	r_e (m)	p_e (MPa)	u (mm)	r_e (m)	p_e (MPa)	u (mm)	r_e (m)	p_e (MPa)	u (mm)
1(a)	0	5.83	1.64	8.40	5.79	1.56	8.35	5.83	1.64	8.40	5.85	1.84	8.22	5.80	1.54	8.44
1(b)	0	5.55	1.64	7.41	5.54	1.60	7.42	5.55	1.64	7.42	5.64	1.84	7.51	5.54	1.60	7.43
1(a)	10	5.83	1.64	8.74	5.79	1.56	8.68	5.83	1.64	8.74	5.85	1.84	8.52	5.80	1.54	8.79
1(b)	10	5.55	1.64	7.55	5.54	1.60	7.57	5.55	1.64	7.57	5.64	1.84	7.68	5.54	1.60	7.59
1(a)	30	5.83	1.64	10.15	5.79	1.56	10.04	5.83	1.64	10.17	5.85	1.84	9.77	5.80	1.54	10.24
1(b)	30	5.55	1.64	8.15	5.54	1.60	8.18	5.55	1.64	8.19	5.64	1.84	8.39	5.54	1.60	8.21
2(a)	0	6.31	0.22	6.16	6.23	0.21	6.07	6.31	0.22	6.16	6.31	0.24	5.99	6.27	0.20	6.21
2(b)	0	5.82	0.22	5.05	5.85	0.21	5.15	5.86	0.22	5.15	5.98	0.24	5.26	5.85	0.21	5.17
2(a)	10	6.31	0.22	6.56	6.23	0.21	6.45	6.31	0.22	6.56	6.31	0.24	6.34	6.27	0.20	6.62
2(b)	10	5.82	0.22	5.21	5.85	0.21	5.32	5.86	0.22	5.32	5.98	0.24	5.46	5.85	0.21	5.35
3(a)	0	19.61	5.79	398.20	16.61	5.62	292.51	19.63	5.79	398.71	16.45	5.40	301.88	19.28	5.51	411.22
3(b)	0	10.82	5.79	110.53	10.76	5.72	111.33	10.88	5.79	111.92	10.44	5.40	112.74	10.82	5.71	113.12
3(a)	10	19.61	5.79	630.72	16.61	5.62	437.21	19.63	5.79	636.09	16.45	5.40	451.93	19.28	5.51	655.76
3(b)	10	10.82	5.79	138.60	10.76	5.72	139.78	10.88	5.79	140.83	10.44	5.40	141.23	10.82	5.71	142.45
4(a)	0	5.19	0.57	2.12	5.18	0.56	2.12	5.19	0.57	2.12	5.21	0.67	2.11	5.18	0.56	2.12
4(b)	0	5.14	0.57	2.08	5.14	0.56	2.08	5.14	0.57	2.08	5.17	0.67	2.08	5.14	0.56	2.08
4(a)	10	5.19	0.57	2.13	5.18	0.56	2.13	5.19	0.57	2.13	5.21	0.67	2.12	5.18	0.56	2.13
4(b)	10	5.14	0.57	2.08	5.14	0.56	2.08	5.14	0.57	2.08	5.17	0.67	2.08	5.14	0.56	2.08
4(a)	30	5.19	0.57	2.16	5.18	0.56	2.16	5.19	0.57	2.16	5.21	0.67	2.15	5.18	0.56	2.16
4(b)	30	5.14	0.57	2.10	5.14	0.56	2.10	5.14	0.57	2.10	5.17	0.67	2.10	5.14	0.56	2.10
5(a)	0	5.99	1.85	6.03	5.94	1.76	5.98	5.99	1.85	6.03	6.01	2.04	5.90	5.96	1.73	6.06
5(b)	0	5.64	1.85	5.17	5.63	1.80	5.17	5.64	1.85	5.18	5.74	2.04	5.26	5.63	1.80	5.18
5(a)	10	5.99	1.85	6.33	5.94	1.76	6.26	5.99	1.85	6.33	6.01	2.04	6.17	5.96	1.73	6.37
5(b)	10	5.64	1.85	5.30	5.63	1.80	5.30	5.64	1.85	5.30	5.74	2.04	5.41	5.63	1.80	5.31
5(a)	30	5.99	1.85	7.60	5.94	1.76	7.48	5.99	1.85	7.62	6.01	2.04	7.32	5.96	1.73	7.69
5(b)	30	5.64	1.85	5.81	5.63	1.80	5.81	5.64	1.85	5.82	5.74	2.04	6.03	5.63	1.80	5.83
6(a)	0	13.33	0.49	76.67	11.75	0.47	60.20	13.32	0.49	76.50	11.74	0.47	60.94	13.04	0.46	77.00
6(b)	0	8.61	0.49	28.82	8.52	0.48	28.54	8.60	0.49	28.70	8.53	0.47	29.68	8.54	0.48	28.78
6(a)	10	13.33	0.49	105.94	11.75	0.47	79.64	13.32	0.49	106.25	11.74	0.47	80.73	13.04	0.46	106.66
6(b)	10	8.61	0.49	33.48	8.52	0.48	33.13	8.60	0.49	33.37	8.53	0.47	34.67	8.54	0.48	33.46
7(a)	0	7.13	0.28	12.44	6.92	0.26	11.80	7.13	0.28	12.43	6.96	0.29	11.50	7.07	0.26	12.57
7(b)	0	6.20	0.28	8.82	6.17	0.27	8.82	6.20	0.28	8.83	6.32	0.29	9.11	6.18	0.27	8.86
7(a)	10	7.13	0.28	13.84	6.92	0.26	13.01	7.13	0.28	13.84	6.96	0.29	12.63	7.07	0.26	14.03
7(b)	10	6.20	0.28	9.26	6.17	0.27	9.26	6.20	0.28	9.27	6.32	0.29	9.63	6.18	0.27	9.31
8(a)	0	27.63	6.23	1178.52	21.74	6.07	749.68	27.63	6.23	1178.02	21.41	5.79	780.55	26.84	5.97	1190.15
8(b)	0	12.73	6.23	230.35	12.58	6.16	228.98	12.75	6.23	230.82	11.94	5.79	225.65	12.67	6.15	233.06
8(a)	10	27.63	6.23	2127.11	21.74	6.07	1239.18	27.63	6.23	2142.97	21.41	5.79	1291.29	26.84	5.97	2152.92
8(b)	10	12.73	6.23	306.05	12.58	6.16	303.91	12.75	6.23	307.29	11.94	5.79	296.56	12.67	6.15	310.38
9(a)	0	24.59	0.58	398.67	18.89	0.57	239.04	24.80	0.58	404.83	19.01	0.55	253.24	22.91	0.56	360.74
9(b)	0	11.36	0.58	77.28	11.17	0.58	75.67	11.29	0.58	76.12	10.90	0.55	76.82	11.22	0.58	76.53
9(a)	10	24.59	0.58	692.52	18.89	0.57	376.44	24.80	0.58	710.96	19.01	0.55	401.69	22.91	0.56	615.96
9(b)	10	11.36	0.58	98.93	11.17	0.58	96.56	11.29	0.58	97.35	10.90	0.55	97.90	11.22	0.58	97.87

Performance estimates have been computed using the parameters for the original HB rock mass and the equivalent MC parameters obtained after linearization with several methods.

^aValues reproduced from [6], who modified the solution provided by [8].

general alternative to the BFe and BFa linearization methods. In Tables 4 and 5 we show that, in general, estimates of performance computed with the proposed method are preferable to estimates of performance computed with the BFe or BFa methods. There are some instances in which the BFe or the BFa methods provide better performance estimates, but that generally occurs for cases in which all methods provide excellent agreement with the real performance of the HB rock mass, often with relative

errors of less than about 1%. However, for cases in which the error is large enough to be of engineering significance (say, more than 10%), our results suggest that the linearization method presented in Section 2 provides better performance estimates than the BFe or the BFa methods.

For instance, plastic radii computed using our linearization method tend to underestimate the size of the plastic zone, with errors in the computed plastic radii of up to 6.8%; whereas the BFe method also tends to

Table 4

Differences (expressed as percentage) between performance estimates of radius of the plastic region, critical pressure, and radial convergence computed using the parameters for the original HB rock mass and the equivalent MC parameters obtained after linearization with several methods

Case	ψ (deg)	Mohr–Coulomb rock mass											
		BF _e			EMR			BF _a			This work		
		δr_e (%)	δp_c (%)	δu (%)	δr_e (%)	δp_c (%)	δu (%)	δr_e (%)	δp_c (%)	δu (%)	δr_e (%)	δp_c (%)	δu (%)
1(a)	0	0.75	4.77	0.60	0.05	-0.24	-0.00	-0.36	-12.02	2.13	0.51	6.06	-0.44
1(b)	0	0.21	2.40	-0.20	-0.06	-0.23	-0.24	-1.63	-12.02	-1.37	0.17	2.65	-0.38
1(a)	10	0.75	4.77	0.71	0.05	-0.24	-0.03	-0.36	-12.02	2.50	0.51	6.06	-0.54
1(b)	10	0.21	2.40	-0.22	-0.06	-0.23	-0.27	-1.63	-12.02	-1.67	0.17	2.65	-0.44
1(a)	30	0.75	4.77	1.11	0.05	-0.24	-0.18	-0.36	-12.02	3.75	0.51	6.06	-0.90
1(b)	30	0.21	2.40	-0.31	-0.06	-0.23	-0.42	-1.63	-12.02	-2.88	0.17	2.65	-0.67
2(a)	0	1.28	5.52	1.43	0.07	0.74	0.01	0.05	-7.09	2.83	0.64	6.83	-0.72
2(b)	0	-0.44	3.03	-1.88	-0.75	0.72	-1.84	-2.70	-7.09	-4.06	-0.50	3.59	-2.27
2(a)	10	1.28	5.52	1.71	0.07	0.74	-0.03	0.05	-7.09	3.32	0.64	6.83	-0.87
2(b)	10	-0.44	3.03	-2.15	-0.75	0.72	-2.11	-2.70	-7.09	-4.85	-0.50	3.59	-2.63
3(a)	0	15.30	2.89	26.54	-0.08	-0.06	-0.13	16.12	6.71	24.19	1.70	4.85	-3.27
3(b)	0	0.54	1.23	-0.72	-0.56	-0.05	-1.26	3.51	6.71	-2.00	-0.03	1.42	-2.34
3(a)	10	15.30	2.89	30.68	-0.08	-0.06	-0.85	16.12	6.71	28.35	1.70	4.85	-3.97
3(b)	10	0.54	1.23	-0.85	-0.56	-0.05	-1.61	3.51	6.71	-1.90	-0.03	1.42	-2.78
4(a)	0	0.17	1.94	-0.01	0.10	-0.54	-0.01	-0.34	-17.47	0.21	0.17	1.96	-0.03
4(b)	0	0.02	0.95	0.01	-0.02	-0.50	0.01	-0.54	-17.47	-0.00	0.02	0.92	0.00
4(a)	10	0.17	1.94	-0.02	0.10	-0.54	-0.02	-0.34	-17.47	0.24	0.17	1.96	-0.04
4(b)	10	0.02	0.95	-0.01	-0.02	-0.50	-0.01	-0.54	-17.47	-0.02	0.02	0.92	-0.02
4(a)	30	0.17	1.94	-0.01	0.10	-0.54	-0.01	-0.34	-17.47	0.42	0.17	1.96	-0.04
4(b)	30	0.02	0.95	0.01	-0.02	-0.50	0.01	-0.54	-17.47	-0.02	0.02	0.92	-0.01
5(a)	0	0.91	4.94	0.88	0.02	-0.13	-0.00	-0.35	-10.11	2.14	0.57	6.52	-0.57
5(b)	0	0.24	2.47	0.02	-0.06	-0.12	-0.02	-1.81	-10.11	-1.71	0.21	2.75	-0.17
5(a)	10	0.91	4.94	1.05	0.02	-0.13	-0.03	-0.35	-10.11	2.52	0.57	6.52	-0.69
5(b)	10	0.24	2.47	0.02	-0.06	-0.12	-0.04	-1.81	-10.11	-2.11	0.21	2.75	-0.21
5(a)	30	0.91	4.94	1.61	0.02	-0.13	-0.26	-0.35	-10.11	3.63	0.57	6.52	-1.17
5(b)	30	0.24	2.47	0.04	-0.06	-0.12	-0.10	-1.81	-10.11	-3.71	0.21	2.75	-0.35
6(a)	0	11.84	3.73	21.48	0.06	0.31	0.22	11.90	5.10	20.52	2.16	5.49	-0.43
6(b)	0	1.07	1.80	0.94	0.09	0.21	0.41	0.98	5.10	-3.00	0.80	1.96	0.11
6(a)	10	11.84	3.73	24.83	0.06	0.31	-0.29	11.90	5.10	23.79	2.16	5.49	-0.68
6(b)	10	1.07	1.80	1.07	0.09	0.21	0.35	0.98	5.10	-3.53	0.80	1.96	0.08
7(a)	0	2.98	5.97	5.11	0.03	1.13	0.08	2.33	-2.75	7.50	0.81	7.73	-1.10
7(b)	0	0.48	3.37	-0.06	0.05	1.19	-0.10	-1.93	-2.75	-3.29	0.36	3.57	-0.48
7(a)	10	2.98	5.97	6.03	0.03	1.13	-0.03	2.33	-2.75	8.76	0.81	7.73	-1.36
7(b)	10	0.48	3.37	-0.07	0.05	1.19	-0.12	-1.93	-2.75	-4.03	0.36	3.57	-0.57
8(a)	0	21.32	2.57	36.39	0.01	0.00	0.04	22.49	7.06	33.77	2.87	4.25	-0.99
8(b)	0	1.16	1.13	0.59	-0.13	-0.01	-0.21	6.22	7.06	2.04	0.46	1.24	-1.18
8(a)	10	21.32	2.57	41.74	0.01	0.00	-0.75	22.49	7.06	39.29	2.87	4.25	-1.21
8(b)	10	1.16	1.13	0.70	-0.13	-0.01	-0.40	6.22	7.06	3.10	0.46	1.24	-1.41
9(a)	0	23.19	2.13	40.04	-0.86	-0.58	-1.55	22.69	5.34	36.48	6.81	2.83	9.51
9(b)	0	1.66	0.61	2.08	0.62	-0.53	1.50	4.06	5.34	0.59	1.20	0.65	0.97
9(a)	10	23.19	2.13	45.64	-0.86	-0.58	-2.66	22.69	5.34	42.00	6.81	2.83	11.06
9(b)	10	1.66	0.61	2.39	0.62	-0.53	1.59	4.06	5.34	1.04	1.20	0.65	1.07

Table 5

Number of test cases (out of a total of 42) in which percentage errors in performance estimates exceed values of 5%, 10%, and 20% for different linearization procedures

Percentage	Mohr–Coulomb rock mass											
	BF _e			EMR			BF _a			This work		
	δr_e (%)	δp_c (%)	δu (%)	δr_e (%)	δp_c (%)	δu (%)	δr_e (%)	δp_c (%)	δu (%)	δr_e (%)	δp_c (%)	δu (%)
5	8	4	10	0	0	0	10	38	10	2	12	2
10	8	0	8	0	0	0	8	18	8	0	0	1
20	4	0	8	0	0	0	4	0	8	0	0	0

underestimate the size of the plastic zone, with errors up to 23% (i.e., more than three times the error of our method). For the 42 cases considered, our method provides only two cases with more than 5% error in the estimation of plastic radius, and zero cases with more than 10% error; whereas the BFe and BFa provide 8 and 10 cases with more than 5% error; eight cases with more than 10% error and four cases with more than 20% error.

Table 6

Sum of squares of relative errors of estimates of plastic radius, critical pressure, and radial convergence when different intermediate cohesion values are considered in the linearization procedure

ζ_c^*	$\sum(\delta r_c)^2$	$\sum(\delta p_c)^2$	$\sum(\delta u)^2$
0.00	5.43E + 01	1.84E - 03	3.66E + 03
0.05	2.31E + 01	1.51E - 03	7.59E + 02
0.10	1.17E + 01	2.33E - 03	2.47E + 02
0.15	6.45E + 00	4.29E - 03	1.00E + 02
0.20	3.69E + 00	7.40E - 03	4.62E + 01
0.25	2.12E + 00	1.17E - 02	2.27E + 01
0.30	1.20E + 00	1.70E - 02	1.14E + 01
0.35	6.46E - 01	2.36E - 02	5.74E + 00
0.40	3.17E - 01	3.13E - 02	2.76E + 00
0.45	1.31E - 01	4.01E - 02	1.20E + 00
0.50	3.69E - 02	5.01E - 02	4.29E - 01
0.55	4.38E - 03	6.12E - 02	1.00E - 01
0.60	1.34E - 02	7.35E - 02	2.82E - 02
0.65	5.07E - 02	8.69E - 02	1.06E - 01
0.70	1.07E - 01	1.01E - 01	2.71E - 01
0.75	1.77E - 01	1.17E - 01	4.84E - 01
0.80	2.55E - 01	1.34E - 01	7.22E - 01
0.85	3.39E - 01	1.52E - 01	9.72E - 01
0.90	4.27E - 01	1.71E - 01	1.22E + 00
0.95	5.17E - 01	1.91E - 01	1.47E + 00
1.00	6.07E - 01	2.13E - 01	1.71E + 00

Our linearization method underestimates radial convergences in some cases and overestimates them in others, with the largest relative errors (of up to 11%) due to underestimation. The BFe and BFa methods also present cases with overestimation and underestimation of convergences, but errors of the BFe and BFa methods are generally significantly larger than errors of our method. For instance, the BFe method provides errors of up to 45% in the estimation of radial convergences, and the BFa method provides errors of up to 42% (i.e., about four times the error of the proposed method). Similarly, our method provides two cases with more than 5% error in the estimation of radial convergence, one case with more than 10% error, and zero cases with more than 20% error; whereas both the BFe and BFa methods provide eight cases with more than 20% error.

The BFe method provides slightly better estimates of the critical pressure value than our method, which still performs better than the BFa method. For the 42 benchmark cases, our method provides 12 cases in which the error in estimation of the critical support pressure lies between 5% and 10%; whereas the BFe method provides four cases within that error interval, and the BFa method provides 38

Table 7

Computed equivalent Mohr–Coulomb parameters for design of the tunnel in two rock masses of different quality

Case	GSI	σ_{ci} (MPa)	m_i	HB rock mass			MC rock mass	
				m_b	s	a	c (kPa)	ϕ (deg)
A	20	5	9.6	0.981	7.30E - 4	0.5	87.3	25.7
B	35	20	10	0.551	1.38E - 4	0.544	111.4	53.2

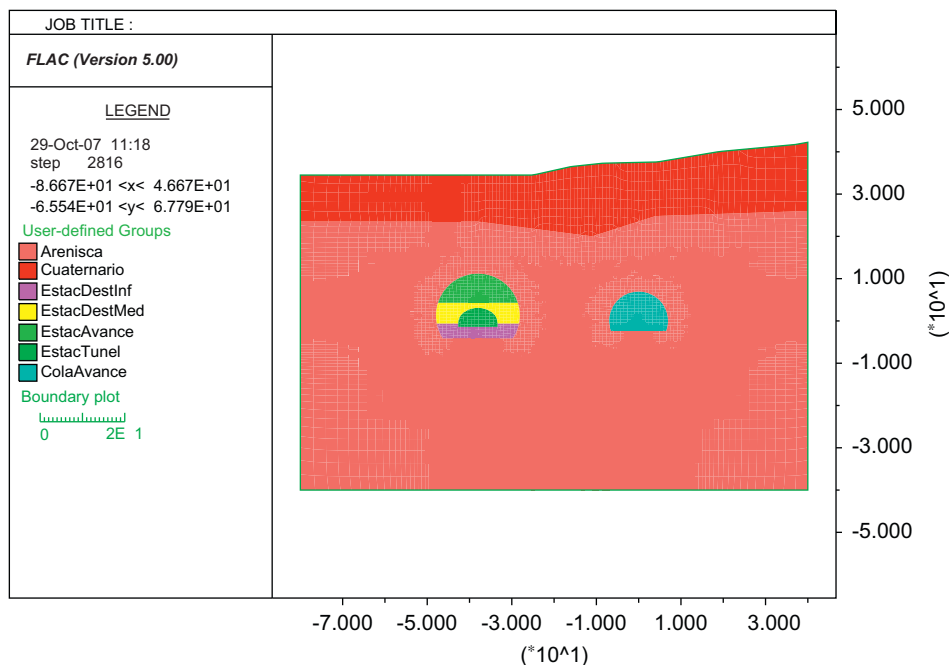


Fig. 4. Geometry of the model.

cases with more than 5% error and 18 with more than 10% error. (Based on the above, however, we believe that this is not a major shortcoming of our method, since it provides less than 10% error for all cases considered; in addition, Sofianos and Nomikos [6] developed simple approximated closed-form expressions to compute the critical pressure in

HB rock masses that reduce the need to compute critical pressures using equivalent MC parameters.)

Finally, we present the results of a sensitivity analysis to assess the value of ξ_C^* in Eq. (7) that provides “optimum” performance estimates. To that end, we use the same 42 benchmark test cases employed above (see e.g., Table 4)

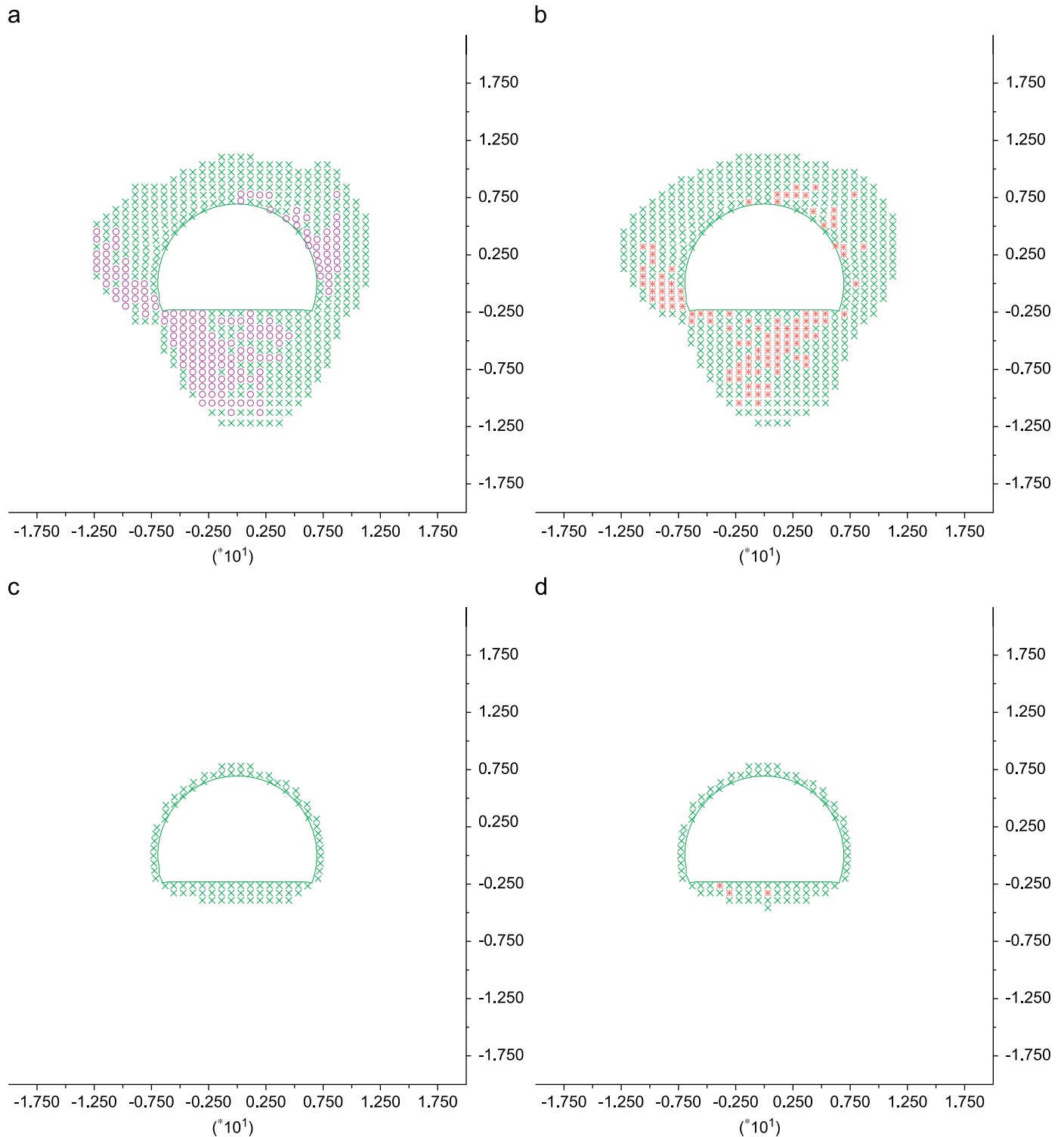


Fig. 5. Plastified region developed around the tunnel for rock masses of different strength, using the original HB strength parameters and the linearized MC strength parameters. (a) Case A; HB rock mass, (b) Case A; MC rock mass, (c) Case B; HB rock mass, (d) Case B; MC rock mass.

and, for each value of ζ_C^* considered, we compute the sum of squares of relative errors (as compared to the performance in the HB rock mass) in estimates of plastic radius, critical pressure, and radial convergence. The results (see Table 6) show that values in the range $0.50 < \zeta_C^* < 0.70$ produce the linearization results that better reproduce the performance of tunnels in the original HB rock mass. Results presented in this paper are computed using $\zeta_C^* = 0.60$.

3.3. Numerical analyses of tunnel response

We have further validated the proposed linearization procedure for tunnelling problems for which analytical solutions are not available. As illustrated in Fig. 4, we have considered an example case of a non-circular tunnel (right) constructed in a fractured rock mass. Such tunnel is to be constructed adjacent to an underground station (left) that is constructed before the tunnel. The station is constructed with the multiple-headings excavation method, whereas the tunnel is constructed using the full-face excavation method. The cross section of the tunnel has a maximum width of 13.8 m and a maximum height of 9.6 m. The tunnel support system consists of a 10 cm thick shotcrete lining and a series of 6 m long passive rock bolts installed in a 2 m × 2 m grid.

A soil formation with $\gamma_{\text{soil}} = 21.1 \text{ kN/m}^3$ unit weight lies on top of the rock mass where the tunnel is constructed. (See Fig. 4.) The rock mass is further considered to have unit weight $\gamma_{\text{rock}} = 26.1 \text{ kN/m}^3$, Poisson's ratio $\nu = 0.3$, and Young's modulus $E_{\text{rock}} = 1850 \text{ MPa}$. The in situ stress is non-hydrostatic, with a ratio of horizontal to vertical stresses of $K_0 = \sigma_h/\sigma_v = 1.5$. Under these conditions, we study the performance of the tunnel described above using the original HB failure criterion and the linearized MC criterion for two rock masses with different strength (but identical stiffness): in Case A we consider one rock mass with $GSI = 20$, $\sigma_{ci} = 5 \text{ MPa}$ and $m_i = 9.6$; and in Case B we consider one rock mass with $GSI = 35$, $\sigma_{ci} = 20 \text{ MPa}$, and $m_i = 10.0$. To that end, we apply the linearization procedure presented in Section 2; this allows us to compute equivalent MC strength parameters that account for the support pressure exerted by the tunnel lining in each case. The results of such linearization procedure are presented in Table 7.

Once the linearization has been completed, we can compare the computed response of the tunnel considering the "original" HB rock mass and the "equivalent" MC rock mass. (Computations have been performed using the explicit finite-difference software FLAC [15].) In that sense, for instance, Fig. 5 shows the plastified region that is formed around the tunnel in each case. It can be observed that, as expected, the plastified region developed around the tunnel is larger for the tunnel constructed in the weaker rock mass (Case A, with $GSI = 20$) than for tunnel constructed in the stronger rock mass (Case B, $GSI = 35$). The results also show that, for a given rock mass, no significant differences in the shape or extension of the plastified zone around the tunnel are found when com-

Table 8

Computed estimates of tunnel response, for rock masses of different strength, using the original HB strength criterion and the linearized MC strength parameters

Case	Type	d_{max} (mm)	T_{max} (kN)	N_{max} (kN/m)	M_{max} (kN · m/m)
A	HB	12.50	74.80	976	17.85
A	MC	12.45	70.18	1001	19.73
B	HB	6.05	7.55	324.1	1.03
B	MC	6.09	7.33	332.8	1.05

Table 9

Differences (expressed as percentage) between computed estimates of tunnel response using the original HB strength criterion and the linearized MC strength parameters

Case	δd_{max} (%)	δT_{max} (%)	δN_{max} (%)	δM_{max} (%)
A	−0.40	−6.17	2.56	10.53
B	0.66	−2.91	2.68	1.94

putations are performed using the linearized MC strength parameters instead of the original HB strength criterion.

We have also computed (and compared) additional aspects of tunnel response that are commonly employed for tunnel design, such as displacements around the tunnel and loads on the tunnel support system. As a summary of such analyses, Table 8 lists the maximum displacement around the tunnel in each case (d_{max}), as well as the maximum load on the rock bolts (T_{max}), and the maximum normal force (N_{max}) and maximum moment (M_{max}) acting on the shotcrete lining. Similarly, Table 9 lists the relative differences between computed estimates of tunnel performance for the rock mass with the original HB strength criterion and for the rock mass with the equivalent MC strength criterion.

Results indicate that, as expected, computed displacements around the tunnel and computed loads on the tunnel support system are larger for weaker rock masses (i.e., Case A, with $GSI = 20$) than for stronger rock masses (i.e., Case B, with $GSI = 35$). Results also show that the relative differences between tunnel response computed with the original HB strength criterion and the linearized MC criterion are not very significant. In that sense, for instance, only the computed estimates of maximum moment for Case A (i.e., with $GSI = 20$) present a relative error of slightly more than 10% between the HB predictions and the MC predictions. In the case of stronger rock masses (i.e., Case B, with $GSI = 35$), results show that the differences in the predictions of support load between the HB rock mass and the MC rock mass are, in all cases, below 3%.

4. Conclusions

We present a new method for estimation of "equivalent" MC strength parameters that can be employed for design of supported tunnels in elasto-plastic rock masses satisfying the generalized HB failure criterion. The linearization

is performed using the adimensional formulation of the HB failure criterion developed by Serrano et al. [13], in which the HB failure criterion is expressed in terms of the normalized Lambe's variables for plane stress. The transformation proposed will remain valid as long as the overall form of the HB criterion is maintained, even if the procedures to compute the parameters of the HB criterion (i.e., m_b , s , and a) change in future versions of the criterion.

The actual stress field in the plastic region around the tunnel is considered, as it is within such plastic region where the rock has reached its ultimate strength. Stresses at the plastic region around the tunnel range from a minimum stress level at the tunnel lining (where the tunnel support pressure represents the minor principal stress) to a maximum stress level at the elasto-plastic interface (where Lambe's p variable remains constant and the radial stress corresponds to the critical pressure).

Results indicate that the actual stress field in the plastic region around the tunnel (including the influence of tunnel support pressure) has a significant impact on computed estimates of equivalent MC strength parameters. The linearization method employed also affects the results. For instance, cohesion values computed with our method tend to be lower than those computed with the BFe and EMR methods, whereas equivalent friction angles computed with our method tend to be higher than those computed with the BFe and EMR methods. (Differences tend to be higher for cases without tunnel support and for cases with lower GSI values.) Relative differences with equivalent MC parameters computed using our method tend to be significantly higher for the BFa method (which does not consider the actual stress field around the tunnel) than for the EMR and BFe methods.

Comparisons of performance predictions computed considering the HB rock mass and considering equivalent MC parameters for different linearization methods have shown that the EMR method provides the smallest relative errors with respect to plastic radius, critical support pressure, and radial convergence. Therefore, following Sofianos and Nomikos [6], we recommend the EMR method to compute equivalent MC strength parameters when the tunnel support pressure is accurately known. However, the EMR is known not to perform well when the estimation of support pressure is poor, as it often happens in real tunnelling projects. In such cases, Sofianos and Nomikos [6] recommend to use the BFe or the BFa methods as an alternative to the EMR method.

In this work we show that our newly introduced linearization methodology can be employed as an alternative to the BFe and BFa methods. We have also validated our linearization procedure using numerical analyses of tunnel response in cases for which analytical solutions are not available. Our results show that our linearization method provides estimates of performance that, in general, are preferable in practice to estimates of performance computed with the BFe or BFa methods. In addition, our results show that the linearization method is

also adequate to estimate loads and moments on the tunnel support system. Even though there are some specific cases in which the BFe or the BFa methods provide better performance estimates, they generally occur when both methods provide excellent agreement with the performance of the HB rock mass and, therefore, when the selection of one method instead of the other does not provide significant practical engineering advantages. Our newly proposed method, however, provides performance estimates that are generally better than performance estimates computed with the BFe or BFa methods in cases in which their difference with the performance of the HB rock mass is of engineering significance (say, more than 10%).

References

- [1] Hoek E, Brown ET. Empirical strength criterion for rock masses. *J Geotech Eng Div ASCE* 1980;106(GT9):1013–35.
- [2] Hoek E, Brown E. The Hoek–Brown failure criterion—a 1988 update. In: Curran J, editor. *Proceedings of the 15th Canadian rock mechanics symposium*. Department Civil Engineering, University of Toronto, 1988. p. 31–8. [Also available from: (<http://www.roscience.com>)].
- [3] Hoek E, Wood D, Shah SA. A modified Hoek–Brown criterion for jointed rock masses. In: Hudson JA, editor. *Proceedings of rock characterization, symposium of the international society of rock mechanics: Eurock 92*. London: British Geotechnical Society; 1992. p. 209–14.
- [4] Hoek E, Brown E. Practical estimates of rock mass strength. *Int J Rock Mech Min Sci* 1997;34(8):1165–86.
- [5] Hoek E, Carranza-Torres C, Corkum B. Hoek–Brown failure criterion—2002 edition, vol. 1. 2002. p. 267–73. [Also available from: (<http://www.roscience.com>)].
- [6] Sofianos AI, Nomikos PP. Equivalent Mohr–Coulomb and generalized Hoek–Brown strength parameters for supported axisymmetric tunnels in plastic or brittle rock. *Int J Rock Mech Min Sci* 2006;43:683–704.
- [7] Park K, Kim Y. Analytical solution for a circular opening in an elastic–brittle–plastic rock. *Int J Rock Mech Min Sci* 2006;43:616–22.
- [8] Carranza-Torres C. Elasto-plastic solution of tunnel problems using the generalized form of the Hoek–Brown failure criterion. *Int J Rock Mech Min Sci* 2004;41(3):480–1. In: Hudson JA, Feng X-T, editors. *Proceedings of the ISRM SINOROCK 2004 symposium*.
- [9] Sharan SK. Analytical solutions for stresses and displacements around a circular opening in a generalized Hoek–Brown rock. *Int J Rock Mech Min Sci* 2008;45(1):78–85.
- [10] Carranza-Torres C. Dimensionless graphical representation of the exact elasto-plastic solution of a circular tunnel in a Mohr–Coulomb material subject to uniform far-field stresses. *Rock Mech Rock Eng* 2003;36(3):237–53.
- [11] Sofianos AI. Tunnelling Mohr–Coulomb strength parameters for rock masses satisfying the generalized Hoek–Brown criterion. *Int J Rock Mech Min Sci* 2003;40:435–40.
- [12] Sofianos AI, Halakatevakis N. Equivalent tunnelling Mohr–Coulomb strength parameters for given Hoek–Brown ones. *Int J Rock Mech Min Sci* 2002;39:131–7.
- [13] Serrano A, Olalla C, Gonzalez J. Ultimate bearing capacity of rock masses based on the modified Hoek–Brown criterion. *Int J Rock Mech Mining Sci* 2000;37:1013–8.
- [14] Duncan Fama M. Numerical modelling of yield zones in weak rocks. In: Hudson JA, editor. *Comprehensive rock engineering, Analysis and design methods*, vol. 2. New York: Pergamon Press; 1993. p. 49–75.
- [15] FLAC 5.0 User's Manual, 2005.